

---

# When Image Denoising Meets High-Level Vision Tasks: A Deep Learning Approach

---

**Ding Liu**

University of Illinois at Urbana-Champaign  
dingliu2@illinois.edu

**Bihan Wen**

University of Illinois at Urbana-Champaign  
bwen3@illinois.edu

**Xianming Liu**

Facebook, Inc.

**Thomas S. Huang**

University of Illinois at Urbana-Champaign  
huang@ifp.uiuc.edu

## Abstract

Conventionally, image denoising and high-level vision tasks are handled separately in computer vision, and their connection is fragile. In this paper, we cope with the two jointly and explore the mutual influence between them with the focus on two questions, namely (1) how image denoising can help solving high-level vision problems, and (2) how the semantic information from high-level vision tasks can be used to guide image denoising. First we propose a deep convolutional neural network for image denoising which is able to outperform the state-of-the-art. Second we propose a deep neural network solution that cascades two modules for image denoising and various high-level tasks, respectively, and propose the use of joint loss for updating only the denoising network to allow the semantic information flowing into the optimization of the denoising network via back-propagation. Our experimental results demonstrate that on one hand, the proposed architecture is able to overcome the performance degradation of different high-level vision tasks, e.g., image classification and semantic segmentation, due to image noise or artifacts caused by conventional denoising approaches such as over-smoothing. On the other hand, with the guidance of high-level vision information, the denoising network can further preserve more fine details and generate more visually appealing results. To the best of our knowledge, this is the first work to systematically investigate the benefit of using high-level vision semantics for image denoising via deep learning.

## 1 Introduction

A common approach in computer vision is to separate low-level vision problems, such as image restoration and enhancement, from high-level vision problems, and solve them independently. In this paper, we show the mutual influence between the two, i.e., visual perception and semantics, and propose a new perspective of solving both the low-level and high-level computer vision problems in a single unified framework. Image denoising, as one representative of low-level vision problems, is dedicated to recovering the underlying image signal from its noisy measurement. When people tackle this problem, the semantical information is usually ignored, which leads to unsatisfactory denoising results. For example, conventional image denoising algorithms usually generate over-smoothing outputs in some texture-rich regions, as shown in Fig. 1 (d). On the other hand, when high-level vision tasks are conducted on noisy data, an independent image restoration step is typically applied as preprocessing, which is suboptimal for the desired task, as illustrated in Section 4.3. Recent research reveals the fact that neural networks trained for image classification can be easily fooled by adding small perturbation or other artificial patterns [17, 13]. However, to the best of our knowledge, there is little study showing how low-level vision processing could affect high-level semantical tasks [19].

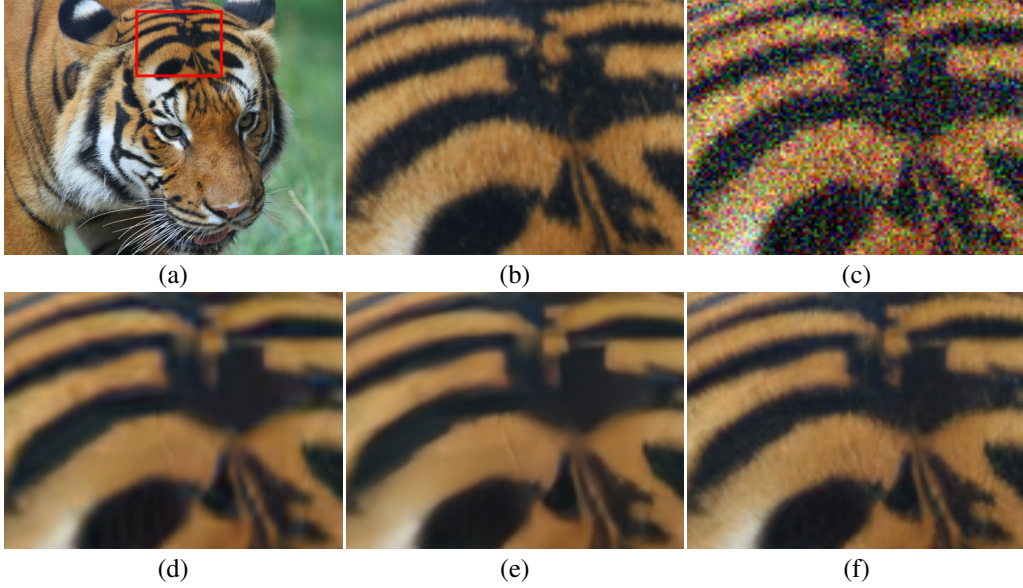


Figure 1: (a) The whole ground truth image  $0100 \times 4$  from DIV2K dataset. We show the comparison of the zoom-in region between: (b) the ground truth; (c) the noisy image with i.i.d. Gaussian noise of zero mean and  $\sigma = 45$ ; (d) the denoised image by BM3D; the denoising result of our proposed denoising network (e) without the guidance of high-level vision information; (f) with the guidance of high-level vision information.

We observe an intriguing result in latter this paper that applying a conventional denoising algorithm such as BM3D [6] onto noisy images introduces lethal artifacts, which undermines the performance of image classification and semantic segmentation.

To this end, we propose a cascade architecture to connect image denoising and high-level semantic tasks in this paper, and systematically investigate the mutual influence between the two. We jointly minimize the pixel-wise image reconstruction loss and the high-level vision loss, in order to simultaneously denoise images and maintain their semantic-aware details for high-level vision tasks. During training, a noisy image goes through a fully convolutional denoising network, followed by a network for high-level task, for instance, VGG [16] for image classification. We keep the high-level task network untouched but only use the loss and gradients to update the denoising network, to make sure the denoising network has good generalization to other high-level vision tasks. This also ensures that denoising not only removes noises but also keeps the semantic information to produce correct high-level vision task results. As for implementation, we propose a convolutional neural network for image denoising. Inspired by U-Net [15], we conduct convolutions in different spatial scales via downsampling and upsampling operations before the resulting features are fused together, so that the kernels have a larger receptive field after all the feature contraction. Downsampling operations also help to reduce the computation cost due to the decrease of the feature map size. The details of the network architecture will be introduced in Section 3.

We conduct a comprehensive evaluation of two modules in our cascade architecture. Our experiments show that our proposed denoising network when trained solely can achieve image denoising results of better quality compared with BM3D, as shown in Fig. 1 (e); with the guidance of high-level vision information, the denoising network is able to further improve the quality and generate more visually appealing outputs, as shown in Fig. 1 (f), which demonstrates the importance of semantic information for image denoising. Meanwhile, by the use of joint loss for training, the high-level vision network in the cascade architecture attains sufficiently good accuracy for high-level vision tasks. Moreover, our proposed training strategy is shown to make the trained denoising network robust enough to different high-level vision tasks. In other words, our denoising module trained for one high-level vision task can be directly plugged into other high-level tasks without finetuning either module, which facilitates the training effort when applied to various high-level tasks and keeps the high-level vision networks performing consistently for noisy and noiseless images. To the best of our knowledge, this is the first work to systematically investigate the mutual influence between image denoising and

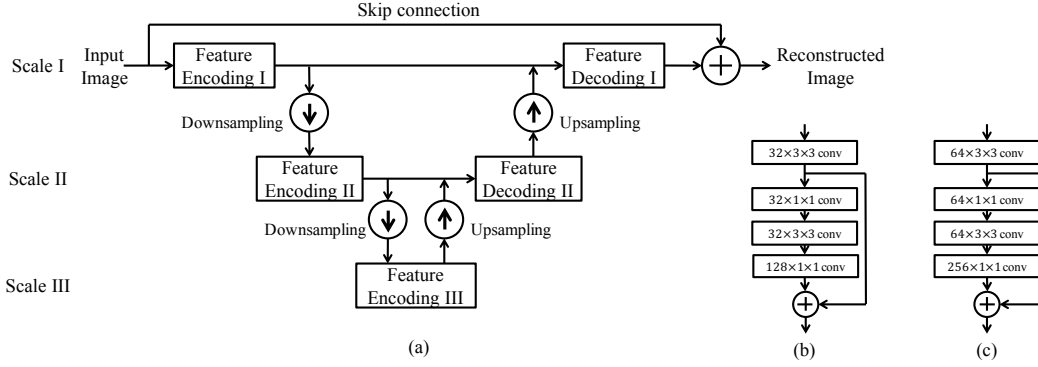


Figure 2: (a) Overview of our proposed denoising network. (b) Architecture of the feature encoding module. (c) Architecture of the feature decoding module.

high-level vision tasks, especially the benefit of using high-level semantics for image denoising via deep learning. Experiment details and source codes are available online<sup>1</sup>.

## 2 Related Work

Denoising is the task of estimating the high-quality signal from its noisy measurements. Classical image denoising methods take advantage of local or non-local structures presented in the image explicitly. Natural images are well-known to be patch-wise sparse or compressible in transform domain, or over certain dictionary. Prior works [2, 20] exploit such local structures and reduce noise by coefficient shrinkage for image restoration. Apart from the image local properties, the later approaches, including SSC [11], CSR [7], GSR [23], STROLLR [21], as well as the well-known BM3D [6] – group similar patches within the image globally via block matching, and impose non-local structural priors on these groups, which usually lead to state-of-the-art image denoising performance.

More recently, the popular deep neural network techniques have been applied to low-level vision tasks. Specifically, a number of deep learning models have been developed for image denoising [18, 9, 3, 22, 12], which can be classified into two categories: multi layer perception (MLP) based models and convolutional neural network (CNN) based models. Early MLP based models for image denoising include the stacked denoising autoencoder [18], which is an extension of the stacked autoencoder originally designed for unsupervised feature learning. A denoising autoencoder is proposed for both image denoising and blind image inpainting by Xie et al. [22]. Burger et al. [3] introduces a plain multilayer perception (MLP) and thoroughly compare its denoising performance with a state-of-the-art denoising algorithm, BM3D [6], in different experimental settings. CNNs are first utilized for image denoising by Jain and Seung [9]. Recently, Mao et al. [12] propose a very deep convolutional autoencoder for image restoration and exploit skip connections for better gradient propagation during training, which achieves superior performance over other recent methods.

## 3 Method

We first introduce the denoising network utilized in our framework, and then explain the relationship between the image denoising module and the module for high-level vision tasks in detail.

### 3.1 Denoising Network

We propose a convolutional neural network for image denoising, which takes a noisy image as input and outputs the reconstructed image. This network conducts feature contraction and expansion through downsampling and upsampling operations, respectively. Each pair of downsampling and upsampling operations divides the feature representation into a new spatial scale, so that the network can process information on different scales.

<sup>1</sup><https://github.com/Ding-Liu/DeepDenoising>

Specifically, on each scale, the input is encoded after downsampling the features from the previous scale. After feature encoding and decoding possibly with features on the next scale, the output is upsampled and fused with the feature on the previous scale. Such pairs of downsampling and upsampling steps can be nested to build deeper networks with more spatial scales of feature representation, which generally leads to better restoration performance. Considering the tradeoff between computation cost and restoration accuracy, we choose three scales for the denoising network in our experiments, while this framework can be easily extended for more scales.

These operations together are designed to learn the residual between the input and the target output and recover as many details as possible, so we use a long-distance skip connection to sum the output of these operations and the input image, in order to generate the reconstructed image. The overview is in Fig. 2 (a). Each module in this network will be elaborated as follows.

**Feature Encoding:** We design one feature encoding module on each scale. which is one convolutional layer plus one residual block as in [8]. The architecture is displayed in Fig. 2 (b). Note that each convolutional layer is immediately followed by spatial batch normalization and a ReLU neuron. From top to down, the four convolutional layers have 32, 32, 32 and 128 kernels in size of  $3 \times 3$ ,  $1 \times 1$ ,  $3 \times 3$  and  $1 \times 1$ , respectively. The output of the first convolutional layer is passed through a skip connection for element-wise sum with the output of the last convolutional layer.

**Feature Decoding:** The feature decoding module is designed for fusing information from two adjacent scales. Two fusion schemes are tested: (1) concatenation of features on these two scales; (2) element-wise sum of them. Both of them obtain similar denoising performance. Thus we choose the first scheme to accommodate feature representations of different channel numbers from two scales. We use a similar architecture as the feature encoding module except that the number of kernels in the four convolutional layers are 64, 64, 64 and 256. Its architecture is in Fig. 2 (c).

**Feature Downsampling & Upsampling:** Downsampling operations are adopted multiple times to progressively increase the receptive field of the following convolution kernels and to reduce the computation cost by decreasing the feature map size. The larger receptive field enables the kernels to incorporate larger spatial context for denoising. We use 2 as the downsampling and upsampling factors, and try two schemes for downsampling in the experiments: (1) max pooling with stride of 2; (2) conducting convolutions with stride of 2. Both of them achieve similar denoising performance in practice, so we use the second scheme in the rest experiments for computation efficiency. Upsampling operations are implemented by deconvolution with  $4 \times 4$  kernels, which aim to expand the feature map to the same spatial size as the previous scale.

Since all the operations in our proposed denoising network are spatially invariant, it has the merit of handling input images of arbitrary size.

### 3.2 When Image Denoising Meets High-Level Vision Tasks

We propose a robust deep architecture processing a noisy image input, via cascading a network for denoising and the other for high-level vision task, aiming to simultaneously:

1. achieve better denoising performance guided by the high-level vision information, as the output of the denoising network;
2. attain sufficiently good accuracy for high-level vision task, as the output of the network for high-level vision task;

The overview of the proposed cascaded network is displayed in Fig. 3. Specifically, given a noisy input image, the denoising network is first applied, and the denoised result is then fed into the following network for high-level vision task, which generates the high-level vision task output. We choose two high-level vision tasks as representatives in our study: image classification and semantic segmentation, which have been dominated by deep network based models. We utilize two popular VGG-based deep networks in our system for each task, respectively. *VGG-16* in [16] is employed for image classification; we select *DeepLab-LargeFOV* in [4] for semantic segmentation.

**Training Strategy:** First we initialize the network for high-level vision task from a network that is well-trained in the noiseless setting. We train the cascade of two networks in an end-to-end manner while fixing the weights in the network for high-level vision task. Only the weights in the denoising network are updated by the error back-propagated from the following network for high-level vision task. The reason to adopt such a training strategy is to make the trained denoising network robust

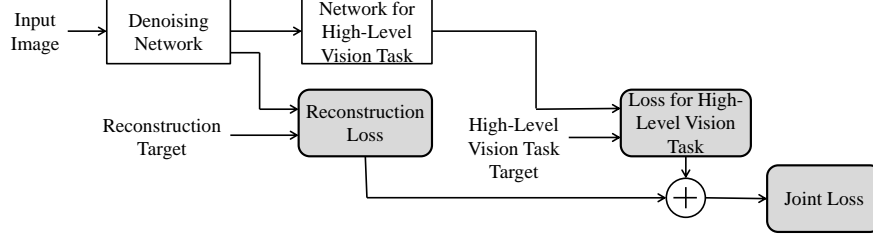


Figure 3: Overview of our proposed cascaded network.

enough without losing the generality for various high-level vision tasks. More specifically, our denoising module trained for one high-level vision task can be directly plugged into other high-level tasks without finetuning either the denoiser or the high-level network. Our approach not only facilitates the training effort when applying the denoiser to different high-level tasks while keeping the high-level vision network performing consistently for noisy and noise-free images, but also enables the denoising network to produce high-quality perceptual and semantically faithful results.

**Loss:** The reconstruction loss of the denoising network is the mean squared error (MSE) between the denoising network output and the noiseless image. The losses of the classification network and the segmentation network both are the cross-entropy loss between the predicted label and the ground truth label. The joint loss is defined as the weighted sum of the reconstruction loss and the loss for high-level vision task, which can be represented as

$$L(F(x), y) = L_D(F_D(x), \tilde{x}) + \lambda L_H(F_H(F_D(x)), y), \quad (1)$$

where  $x$  is the noisy input image,  $\tilde{x}$  is the noiseless image and  $y$  is the ground truth label of high-level vision task.  $F_D$ ,  $F_H$  and  $F$  denote the denoising network, the network of high-level vision task and the whole cascaded network, respectively.  $L_D$ ,  $L_H$  represent the losses of the denoising network and the high-level vision task network, respectively, while  $L$  is the joint loss, as illustrated in Fig. 3.  $\lambda$  is the weight for balancing the losses  $L_D$  and  $L_H$ .

## 4 Experiments

### 4.1 Implementation Details

Our proposed denoising network takes RGB images as input, and outputs the reconstructed images of three channels directly. We download the *VGG-16* model in [16] and the *DeepLab-LargeFOV* model in [4] from the authors' websites. We follow the preprocessing protocols (e.g. crop size, mean removal of each color channel) in [16] and [4] accordingly while training and deploying them with the denoising network for our experiment. We add independent and identically distributed Gaussian noise with zero mean to the original image as the noisy input image of our proposed cascaded network. We train a different denoising network for each noise level in our experiment (i.e.,  $\sigma = 15, 30, 45$ , and 60). Our implementation is based on Caffe [10], and we run our experiments using one NVIDIA Pascal Titan X GPU.

As for the cascaded network for image classification and the corresponding experiments, we train our model on ILSVRC2012 training set, which contains around 1.2 million images, and evaluate the classification accuracy on 50,000 images in ILSVRC2012 validation set. In training, we use stochastic gradient descent (SGD) with a batch size of 10. The initial learning rate is set as  $10^{-5}$  and is divided by 10 after every 80,000 iterations. The training is terminated after 200,000 iterations.  $\lambda$  is set as  $2.5 \times 10^3$ .

As for the cascaded network for image semantic segmentation and its corresponding experiments, we train our model on the augmented training set of Pascal VOC 2012 as in [4], which has 10,582 fully labeled images. Similarly, we use the 1,449 images in the validation set of Pascal VOC 2012 as in [4] to measure the semantic segmentation performance. In training, we use SGD with a batch size of 6. The initial learning rate is set as  $10^{-3}$  and is divided by 5 after every 12,000 iterations. The training is terminated after 60,000 iterations.  $\lambda$  is set as  $5 \times 10^4$ .

Besides the cascaded networks, we separately train a denoising network over the training set of 10,582 images as in [4], in order to compare the denoising results with and without the guidance of high-level vision information. The loss of training is equivalent to Eqn. 1 as  $\lambda = 0$ . We use SGD with a batch

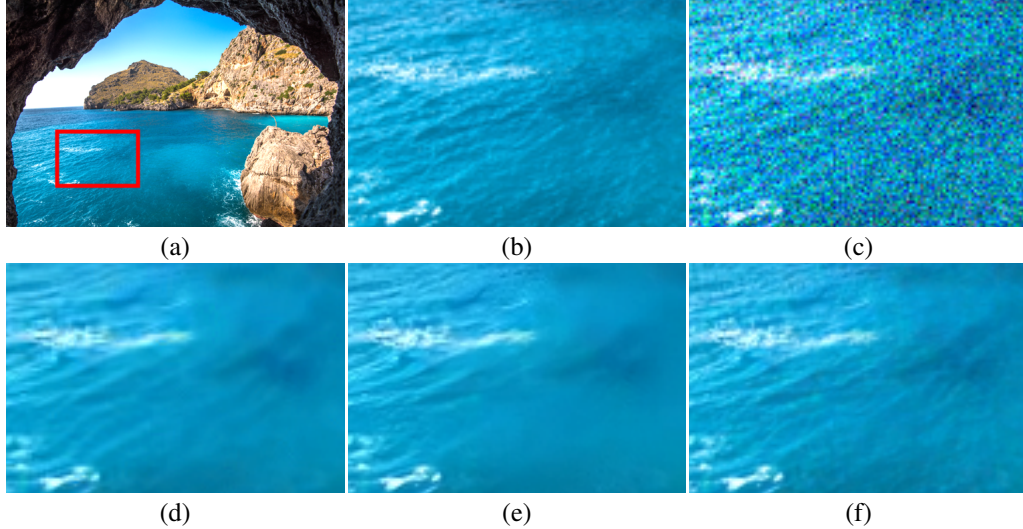


Figure 4: (a) The whole ground truth image *0051x4* from DIV2K dataset. We show the comparison of the zoom-in region between: (b) the ground truth; (c) the noisy image with i.i.d. Gaussian noise of zero mean and  $\sigma = 30$ ; (d) the denoised image by BM3D; the denoising result of our proposed denoising network (e) without the guidance of high-level vision information; (f) with the guidance of high-level vision information.

$\sigma$	Online TL	EPLL	BM3D	Separate Training	Joint Training
15	31.90	31.47	33.07	33.40	33.08
30	27.81	27.88	29.67	30.29	30.01
45	25.44	26.08	27.80	28.50	28.26
60	24.37	24.92	26.59	27.31	27.07

Table 1: PSNR values (in dB) for image denoising, averaged over 1,449 images in Pascal VOC 2012 validation set (task: semantic segmentation). **Red** is the best and **blue** is the second best results.

size of 64. The initial learning rate is set as  $10^{-4}$  and is divided by 10 after every 10,000 iterations. The training is terminated after 30,000 iterations.

## 4.2 High-Level Vision Information Guided Image Denoising

We demonstrate the image denoising results using the proposed denoising network and other competing methods. We measure the peak signal-to-noise ratio (PSNR) in decibel (dB), which is computed between the reference image and the denoised output. The PSNRs of each denoising method are calculated over the validation set of ILSVRC2012 and Pascal VOC 2012, respectively. In order to further compare the denoising network with and without the guidance of high-level vision information, we evaluate the denoising performance on the training set of a newly collected dataset *DIV2K* [1], containing 800 images in the lossless PNG format, which are more preferable for benchmarking different denoising algorithms, while the images of the validation set of ILSVRC2012 and Pascal VOC 2012 are in the lossy JPEG format. We use the version of x4 bicubic downscaling in DIV2K dataset due to its high quality and rich textures.

Fig. 4 demonstrates an image denoising example. A visual comparison is illustrated for a zoom-in region: Fig. 4 (d) and Fig. 4 (e) are the denoised results using the state-of-the-art BM3D [5], and the proposed denoising network trained separately without the guidance of high-level vision information, respectively; Fig. 4 (f) is the denoised result using the proposed denoising network which is trained jointly with the guidance. Both the results using BM3D and separately trained denoising network generate oversmoothing regions, while the jointly trained denoising network is able to provide the

$\sigma$	online TL	EPLL	BM3D	Separate Training	Joint Training
15	31.67	31.28	32.73	33.01	32.81
30	27.53	27.70	29.22	29.71	29.51
45	25.17	25.82	27.34	27.84	27.67
60	23.53	24.57	26.08	26.58	26.41

Table 2: PSNR values (in dB) for image denoising, averaged over 800 images in DIV2K dataset (high-level task: semantic segmentation). **Red** is the best and **blue** is the second best results.

$\sigma$	Online TL	EPLL	BM3D	Separate Training	Joint Training
15	31.50	31.09	32.58	32.96	32.88
30	27.67	27.87	29.39	29.83	29.71
45	25.49	25.95	27.50	28.03	27.96
60	23.78	24.58	26.17	26.79	26.68

Table 3: PSNR values (in dB) for image denoising, averaged over 50,000 images in ILSVRC2012 validation dataset (task: image classification). **Red** is the best and **blue** is the second best results.

denoised image which preserves more details and textures, providing better visual quality. We observe similar visual quality improvement in other denoised results, e.g., the visual example in Fig. 1.

Table 1 shows the average denoising PSNRs (in dB) using different methods, including the online transform learning (online TL) [14], the EPLL<sup>2</sup> [24], the BM3D [6], as well as the methods using our denoising network (i.e., separate training and joint training). It is clear that our proposed methods, with or without high-level vision guidance, outperform the conventional approaches quantitatively. Though the denoised results using the jointly trained network provide lower average PSNR, comparing to those using the separately trained network, they usually have less undesired artifacts (e.g., oversmoothing), with the help of the high-level vision information.

Table 2 and Table 3 list the average denoising PSNRs when we extend the denoising experiments to DIV2K and ILSVRC2012 validation datasets, where the similar improvements are observed. Moreover, even if running in CPU, our denoising network costs much less inference time than all the competing methods.

### 4.3 Enhancing High-Level Vision Task Performance by Data-Driven Denoising

We now investigate how the image denoising can enhance the high-level vision applications, including image classification and semantic segmentation, over the ILSVRC2012 and Pascal VOC 2012 datasets, respectively. The noisy images ( $\sigma = 30$ ) are denoised and then fed into the VGG-based networks for high-level vision tasks. To evaluate how different denoising schemes contribute to the performance of high-level vision tasks, we experiment with the following cases:

<sup>2</sup>We denoise each color channel using the grayscale image denoising implementation which is publicly available at the authors' website.

	VGG	BM3D + VGG	Separate + VGG	Single Loss	Joint Training	Joint Training (Cross Task)
PSNR	N/A	29.39	29.79	29.04	29.71	29.59
Top-1 Accuracy (%)	44.4	62.3	62.7	67.1	67.0	66.4
Top-5 Accuracy (%)	68.9	84.8	84.9	87.7	87.6	87.2

Table 4: Classification accuracy and PSNR values for denoising noisy image ( $\sigma = 30$ ), averaged over 50,000 images in ILSVRC2012 validation dataset. **Red** is the best and **blue** is the second best results.



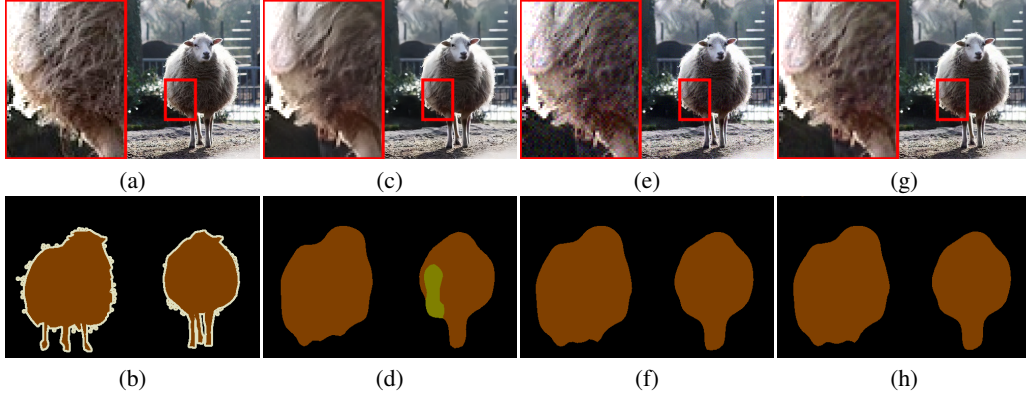


Figure 5: The ground truth of (a) the image 2007\_000925 from Pascal VOC 2012 validation set, and (b) the segmentation labels. We show the comparison of the denoised images (resp. the segmentation results) using (c) the separately trained denoiser (resp. (d)), (e) the coupled denoiser trained using only segmentation network loss (resp. (f)), and (g) the coupled denoiser trained using the denoising and segmentation joint loss (resp. (h)). The zoom-in region which generates inaccurate segmentation in (d) is displayed in the red box.

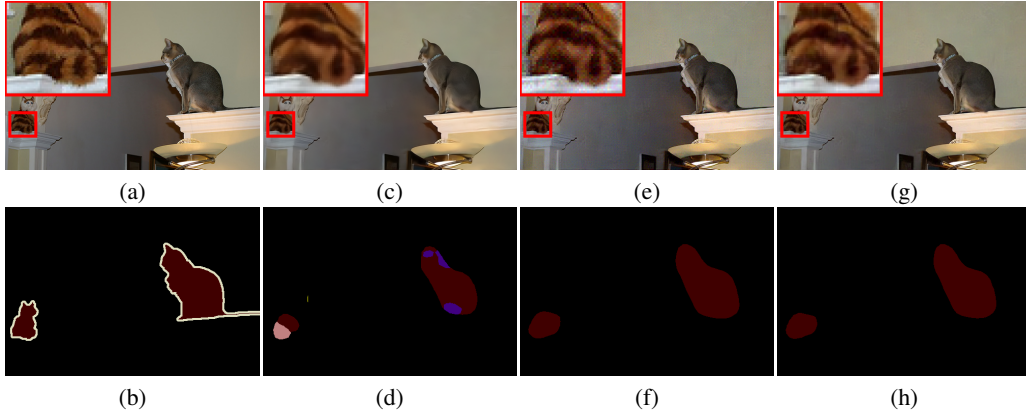


Figure 6: The ground truth of (a) the image 2010\_001913 from Pascal VOC 2012 validation set, and (b) the segmentation labels. We show the comparison of the denoised images (resp. the segmentation results) using (c) the separately trained denoiser (resp. (d)), (e) coupled denoiser trained using only segmentation network loss (resp. (f)), and (g) the coupled denoiser trained using the denoising and segmentation joint loss (resp. (h)). The zoom-in region which generates inaccurate segmentation in (d) is displayed in the red box.

- noisy images are directly fed into the high-level vision network, termed as *VGG*. This approach serves as the baseline;
- noisy images are first denoised by BM3D, and then fed into the high-level vision network, termed as *BM3D+VGG*;
- noisy images are denoised via the separately trained denoising network, and then fed into the high-level vision network, termed as *Separate+VGG*;

	VGG	BM3D + VGG	Separate + VGG	Single Loss	Joint Training	Joint Training (Cross Task)
PSNR	N/A	29.67	30.29	27.13	30.01	30.12
mIoU (%)	43.43	55.29	54.13	57.94	57.86	55.31

Table 5: Semantic segmentation accuracy and PSNR values for denoising noisy image ( $\sigma = 30$ ), averaged over 1,449 images in Pascal VOC 2012 validation dataset. **Red** is the best and **blue** is the second best results.



- noisy images are processed by the cascade of the denoising network and high-level vision network, which is trained using only the loss of high-level vision task, termed as *Single Loss*;
- our proposed approach: noisy images are processed by the cascade of these two networks, which is trained using the joint loss, termed as *Joint Training*.
- a denoising network is trained with the classification network in our proposed approach, but then is connected to the segmentation network, or vice versa. This is to validate the generality of our denoiser for various high-level tasks, termed as *Joint Training (Cross Task)*.

Note that the weights in the high-level vision network are initialized from a well-trained network under the noiseless setting and not updated during training in our experiments.

Table 4 and Table 5 list the performance of high-level vision tasks, i.e., top-1 and top5 accuracies for classification and mean intersection-over-union (IoU) without conditional random field (CRF) postprocessing for semantic segmentation. We notice that the baseline VGG approach obtains much lower accuracy than all the other cases, which shows the necessity of image denoising as a preprocessing step for high-level vision tasks on noisy data. When we only apply denoising without considering high-level semantics (e.g., in BM3D+VGG and Separate+VGG), it also fails to achieve high accuracy due to the artifacts introduced by denoisers. The proposed Joint Training approach achieves sufficiently high accuracies, while generating the denoising results with comparable PSNRs to those in Separate+VGG, which are the highest.

As for the case of Joint Training (Cross Task), first we train the denoising network jointly with the segmentation network and then connect this denoiser to the classification network. As shown in Table 4, its accuracy remarkably outperforms the cascade of a separately trained denoising network and a classification network (i.e., Separate+VGG), and is comparable to our proposed model dedicatedly trained for classification (Joint Training). In addition, we use the denoising network jointly trained with the classification network, to connect the segmentation network. Its mean IOU is much better than Separate+VGG in Table 5. These two experiments show the high-level semantics of different tasks are universal in terms of low-level vision tasks, which is in line with intuition, and the denoiser trained in our method has the generality for various high-level tasks.

Fig. 5 displays one visual example of how the data-driven denoising can enhance the semantic segmentation performance. It is observed that the segmentation result of the denoised image from the separately trained denoising network has lower accuracy compared to those using single or joint loss, while the zoom-in region of its denoised image for inaccurate segmentation in Fig. 5 (c) contains the over-smoothing artifacts. Although both the Single Loss approach and Joint Training approach attain the highest segmentation accuracy, the Single Loss approach produces much poorer denoising results with severe artifacts than the Joint Training approach does. Another visual example is shown in Fig. 6 with the similar observation.

## 5 Conclusion and Future Work

Exploring the connection between low-level vision and high level semantic tasks is essential in various applications of computer vision. It provides a feasible solution to build robust and generalized methodology to real world problems. In this paper, we attack this challenge in a simple yet efficient way by allowing the high-level semantic information passing down the the low-level vision part, which achieves superior performance in both image denoising and various high-level vision tasks. Another advantage of the proposed method is that it is generalized enough to be applied to other tasks. For future work, we will explore to embed the high-level semantics to more low-level vision tasks, as well as bringing more types of semantical information into consideration.

## References

- [1] <https://competitions.codalab.org/competitions/16305>.
- [2] M. Aharon, M. Elad, and A. Bruckstein. K-SVD : An algorithm for designing overcomplete dictionaries for sparse representation. *IEEE Transactions on Signal Processing*, 54(11):4311–4322, 2006.
- [3] H. C. Burger, C. J. Schuler, and S. Harmeling. Image denoising: Can plain neural networks compete with bm3d? In *Computer Vision and Pattern Recognition (CVPR), 2012 IEEE Conference on*, pages 2392–2399. IEEE, 2012.

- [4] L.-C. Chen, G. Papandreou, I. Kokkinos, K. Murphy, and A. L. Yuille. Semantic image segmentation with deep convolutional nets and fully connected crfs. *arXiv preprint arXiv:1412.7062*, 2014.
- [5] K. Dabov, A. Foi, V. Katkovnik, and K. Egiazarian. Color image denoising via sparse 3d collaborative filtering with grouping constraint in luminance-chrominance space. In *Image Processing, 2007. ICIP 2007. IEEE International Conference on*, volume 1, pages I–313. IEEE, 2007.
- [6] K. Dabov, A. Foi, V. Katkovnik, and K. Egiazarian. Image denoising by sparse 3-d transform-domain collaborative filtering. *IEEE Transactions on image processing*, 16(8):2080–2095, 2007.
- [7] W. Dong, X. Li, L. Zhang, and G. Shi. Sparsity-based image denoising via dictionary learning and structural clustering. In *IEEE Conf. Comput. Vision and Pattern Recognition (CVPR 2011)*, pages 457–464, June 2011.
- [8] K. He, X. Zhang, S. Ren, and J. Sun. Deep residual learning for image recognition. In *Proceedings of the IEEE Conference on Computer Vision and Pattern Recognition*, pages 770–778, 2016.
- [9] V. Jain and S. Seung. Natural image denoising with convolutional networks. In *Advances in Neural Information Processing Systems*, pages 769–776, 2009.
- [10] Y. Jia, E. Shelhamer, J. Donahue, S. Karayev, J. Long, R. Girshick, S. Guadarrama, and T. Darrell. Caffe: Convolutional architecture for fast feature embedding. In *Proceedings of the 22nd ACM international conference on Multimedia*, pages 675–678. ACM, 2014.
- [11] J. Mairal, F. Bach, J. Ponce, G. Sapiro, and A. Zisserman. Non-local sparse models for image restoration. In *IEEE 12th Int. Conf. Comput. Vision (ICCV 2009)*, pages 2272–2279, Sept 2009.
- [12] X. Mao, C. Shen, and Y.-B. Yang. Image restoration using very deep convolutional encoder-decoder networks with symmetric skip connections. In *Advances in Neural Information Processing Systems 29*, pages 2802–2810. 2016.
- [13] A. Nguyen, J. Yosinski, and J. Clune. Deep neural networks are easily fooled: High confidence predictions for unrecognizable images. In *Proceedings of the IEEE Conference on Computer Vision and Pattern Recognition*, pages 427–436, 2015.
- [14] S. Ravishanker, B. Wen, and Y. Bresler. Online sparsifying transform learning—part i: Algorithms. *IEEE Journal of Selected Topics in Signal Processing*, 9(4):625–636, 2015.
- [15] O. Ronneberger, P. Fischer, and T. Brox. U-net: Convolutional networks for biomedical image segmentation. In *International Conference on Medical Image Computing and Computer-Assisted Intervention*, pages 234–241. Springer, 2015.
- [16] K. Simonyan and A. Zisserman. Very deep convolutional networks for large-scale image recognition. *arXiv preprint arXiv:1409.1556*, 2014.
- [17] C. Szegedy, W. Zaremba, I. Sutskever, J. Bruna, D. Erhan, I. Goodfellow, and R. Fergus. Intriguing properties of neural networks. *arXiv preprint arXiv:1312.6199*, 2013.
- [18] P. Vincent, H. Larochelle, Y. Bengio, and P.-A. Manzagol. Extracting and composing robust features with denoising autoencoders. In *Proceedings of the 25th international conference on Machine learning*, pages 1096–1103. ACM, 2008.
- [19] Z. Wang, S. Chang, Y. Yang, D. Liu, and T. S. Huang. Studying very low resolution recognition using deep networks. In *Proceedings of the IEEE Conference on Computer Vision and Pattern Recognition*, pages 4792–4800, 2016.
- [20] B. Wen, S. Ravishanker, and Y. Bresler. Structured overcomplete sparsifying transform learning with convergence guarantees and applications. *Int. Journal of Computer Vision*, 114(2-3):137–167, 2015.
- [21] B. Wen, S. Ravishanker, and Y. Bresler. When sparsity meets low-rankness: Transform learning with non-local low-rank constraint for image restoration. In *IEEE Int. Conf. on Acoustics, Speech and Signal Processing (ICASSP)*, 2017.
- [22] J. Xie, L. Xu, and E. Chen. Image denoising and inpainting with deep neural networks. In *Advances in Neural Information Processing Systems*, pages 341–349, 2012.
- [23] J. Zhang, D. Zhao, and W. Gao. Group-based sparse representation for image restoration. *IEEE Transactions on Image Processing*, 23(8):3336–3351, 2014.
- [24] D. Zoran and Y. Weiss. From learning models of natural image patches to whole image restoration. In *Computer Vision (ICCV), 2011 IEEE International Conference on*, pages 479–486. IEEE, 2011.